Energy spectrum of multi-radiation of X-rays in a low energy Mather-type plasma focus device

Farzin M. Aghamir† and Reza A. Behbahani

Department of Physics, University of Tehran, N. Kargar Ave., Tehran 143399, *Iran*

(Received 27 October 2013; revised manuscript received 11 January 2014; published online 10 April 2014)

The multi-radiation of X-rays was investigated with special attention to their energy spectrum in a Mather-type plasma focus device (operated with argon gas). The analysis is based on the effect of anomalous resistances. To study the energy spectrum, a four-channel diode X-ray spectrometer was used along with a special set of filters. The filters were suitable for detection of medium range X-rays as well as hard X-rays with energy exceeding 30 keV. The results indicate that the anomalous resistivity effect during the post pinch phase may cause multi-radiation of X-rays with a total duration of 300 ± 50 ns. The significant contribution of Cu–Kα was due to the medium range X-rays, nonetheless, hard X-rays with energies greater than 15 keV also participate in the process. The total emitted X-ray energy in the forms of Cu–K$_\alpha$ and Cu–K$_\beta$ was around 0.14 ± 0.02 (J/Sr) and 0.04 ± 0.01 (J/Sr), respectively. The total energy of the emitted hard X-ray (> 15 keV) was around 0.12 ± 0.02 (J/Sr).

Keywords: Mather-type plasma focus device, hard X-rays, multi-radiation, tube multiple voltage peaks, anomalous resistances

PACS: 52.58.Lq, 52.59.Px, 52.70.La, 33.20.Rm **DOI:** 10.1088/1674-1056/23/6/065203

1. Introduction

A short-lived (50 ns–100 ns), high-temperature, and high density compressed plasma is produced in a variety of plasma focus (PF) devices by a strong and self-generated magnetic field. The PF devices can emit intensive ion- and electron-beams,[1–5] soft and hard X-rays,[6–9] and neutron beams.[10] The radiation and emission from these plasmas have a wide range of applications in many fields such as pulsed activation analysis through the use of neutrons,[11] lithography, micro-lithography, and microscopy.[12–14]

There are two well-known mechanisms for X-ray radiation in plasma focus (PF) devices: line and continuum radiation. The line radiation has two scenarios: origination from the vacuum vessel working gas medium and the interaction between the energetic electrons and the anode. The anode is usually made of copper; thus the dominant line radiation is Cu–K$_\alpha$.[15–18] The total radiated energy from the second process exceeds the energy from the first one.

The continuum radiation in plasma focus machines includes recombination and Bremsstrahlung. The latter is caused by the acceleration of electrons in a Coulomb field of ions. This can also produce hard X-rays.

One of the attractive aspects of X-ray radiation in plasma focus devices is related to the X-ray emission from the interaction of energetic electrons with the anode tip. Zakaullah *et al.* performed a number of experiments on X-ray radiation in Mather-type PF devices.[18–23] The experiments were based on the interaction of energetic electrons with the anode tip. The effects of many parameters such as the charging voltage, filling gas pressure, anode tip material, anode geometry, and pre ionization system were considered in those experiments. Based on X-ray imaging, anisotropy of X-ray radiation due to the interaction of electrons with the anode tip, and time resolved studies of X-ray production, the energy of the X-ray radiation can be estimated. Zakaullah *et al.* reported the production of hard X-rays with energy more than 15 keV and 15 ns–20 ns pulse duration. The hard X-rays are produced by the interaction of the e-beam, generated in the focus region, with the center of the anode tip.[24] They also speculated that the contribution for Cu–K$_\alpha$ emission by the energetic electron beam generated in the focus region is not significant, whereas the energetic discharge electrons in the current sheath contribute significantly to Cu–K$_\alpha$ emission. These experiments showed that the duration of Cu–K$_\alpha$ emission is on the order of 60 ns and its source size is in the order of anode radius.[18,19]

In both Fillipov- and Mather-type PF devices, the mechanism of X-ray generation is due to the interaction of energetic electrons with the anode surface. Fillipov also reported a discharge mode that causes explosive surface evaporation and hard X-ray emission with energy close to 50 keV without formation of a dense plasma column. This is in accord with the Vikhrev theory that considers the Hall effect near the anode surface.[25]

In the present article, the energy spectrum of multi-radiation of X-rays and in particular, the portion that is related to the X-ray produced by the interaction of energetic electrons with the anode surface has been studied. Based on Lee's model with the anomalous resistance effect included, the

†Corresponding author. E-mail: aghamir@ut.ac.ir

© 2014 Chinese Physical Society and IOP Publishing Ltd

simultaneous occurrence of multi-radiation of X-rays with the multi-peak feature of the tube voltage during the long decrease of plasma current in the radial phase, has been discussed. The study also includes an analysis of the energy spectrum of multi-radiation of X-rays together with its contribution during the radiation process, using a four-channel diode X-ray spectrometer (DXS) and suitable X-ray filters.[26]

2. Experimental set up

The experiments were carried out in a low energy (up to 4.9 kJ) Mather-type plasma focus system operated with argon gas (See Fig. 1). The central electrode (anode) was a conventional cylindrical oxygen-free high conductivity copper rod with a length and radius of 13 cm and 1 cm, respectively. Six copper rods, 12-cm long and 0.9 cm in diameter, were placed symmetrically around the anode. This configuration formed a 3-cm radius cathode in such a way that the radius ratio of the cathode assembly to the anode was 3. Each of the six electrodes was screwed to a copper cathode base plate. A 0.25-cm thick Pyrex insulator sleeve with a radius of 1.25 cm was used to separate the anode from the cathode base at the bottom. The entire anode-cathode assembly was placed inside a stainless steel chamber and a mechanical two-stage vacuum pump was used to evacuate the chamber.

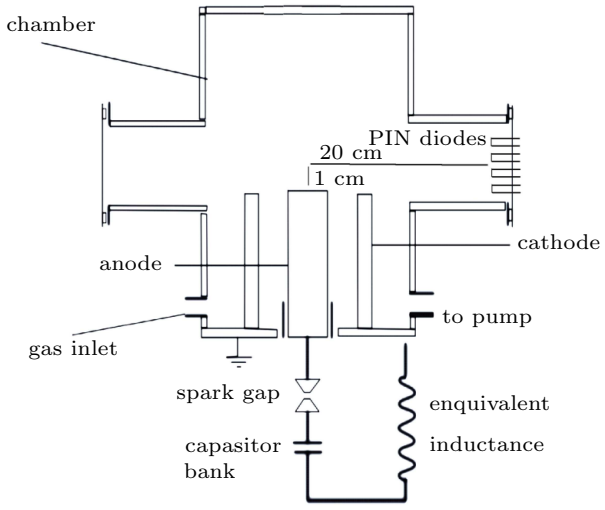


Fig. 1. Schematic illustration of the experimental setup along with positions of PIN diodes.

To record the discharge current, a calibrated Rogowski coil equipped with an appropriate integrator was used. A Tektronix P6015A high voltage probe monitored the tube voltage. Time resolved radiation of X-rays and their energy spectrum was studied by a four-channel diode X-ray spectrometer (DXS). This included four windowless silicon PIN diodes (BPX65) with a wide spectral range and fast response time (Fig. 2), along with suitable absorption filters. All four PIN-diodes were cross-calibrated using the same filters. These detectors were placed in the side-on direction at 20 ± 0.5 cm from the anode axis. They were elevated to 1 ± 0.5 cm from the anode tip. All of the signals were transferred by three-meter long equal-length 50-Ω coaxial cables and recorded by a four–channel, 100 MHz, 1 GSP digital Tektronix oscilloscope. A schematic plot of the experimental set up is shown in Fig. 1.

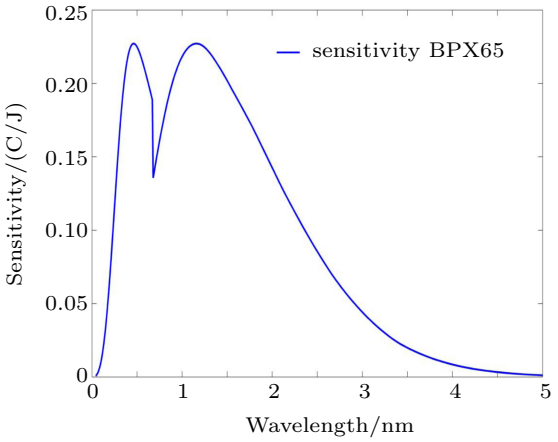


Fig. 2. (color online) Response curve of the BPX65 PIN diode detector.

A simple method using a set of filters along with PIN-diode detectors was conducted[26] to analyze the energy spectrum of the X-rays. The filters included Cu (15 μm), Co (15 μm), Ni (15 μm), and Al (2000 μm). In some shots, Pb (150 μm) replaced Al (2000 μm). Figures 3(a) and 3(b) show transmission curves of the filters and the detectors' responses, respectively.[27,28] The detector masked with a Cu filter allows transmission of X-rays in the 4 keV–9 keV energy range and has the highest transmission response in the energy range that includes the Cu–K_α (8.05 keV) and Cu–K_β (8.9 keV) lines. Therefore, it is a suitable detector for receiving the X-rays in this range of energy. The detector masked with a Co filter provides a window for X-rays in the 4 keV–7.7 keV energy range. The k-edge of Co lies at 7.7 keV, so it absorbs Cu–K_α X-rays and significantly discriminates against Cu–K_β. The detector masked with Ni gives a window in the energy range of 4 keV–8.33 keV with k-edge at 8.33 keV, and the detector transmits Cu–K_α, whereas it absorbs Cu–K_β. The detector masked with an Al filter absorbs X-rays below the energy range of 15 keV. When it is masked with Pb, it detects X-rays in the energy range above 30 keV. The comparison of the intensities (areas under the curves) gained by the detectors masked with Cu, Co, and Ni, demonstrates the contribution of Cu–K_α and Cu–K_β in the X-rays radiated by plasma, whereas a detector masked with Al or Pb detects X-rays with energies exceeding 15 keV and 30 keV, respectively. This set of filters has been selected to provide relevant information on the X-ray transmission that comes from the interaction of energetic electrons with the anode tip.

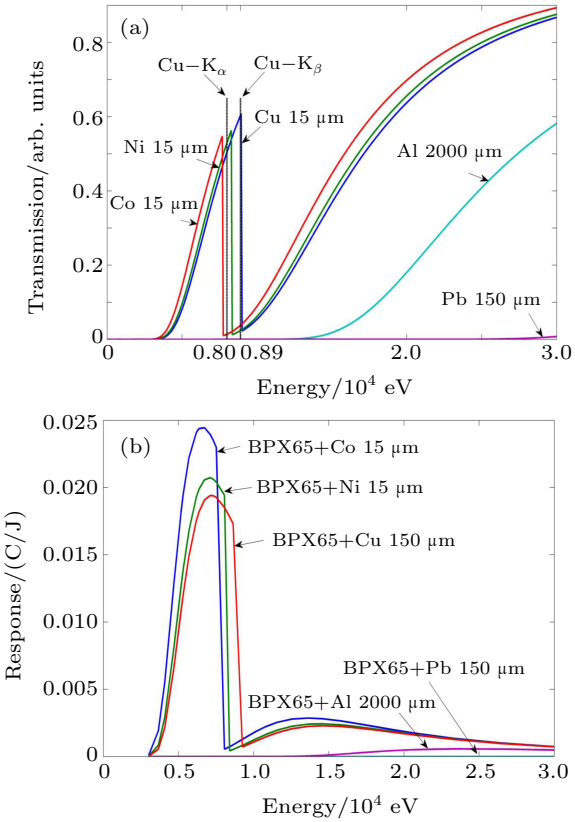


Fig. 3. (color online) (a) Transmission curves of Co (15 μm), Ni (15 μm), Cu (15 μm), Al (2000 μm), and Pb (150 μm) filters. (b) Response curves of the BPX-65 PIN diode masked with Co (15 μm), Ni (15 μm), Cu (15 μm), Al (2000 μm), and Pb (150 μm) filters

3. Experimental results

In this study, argon was used as the filling gas in the pressure range of 0.2 mbar–2 mbar (1 bar = 10^5 Pa) and the charging voltage was set between 15 kV–20 kV. In most of the experimental runs, especially in the low range of operating pressure (0.2 mbar–0.8 mbar), the current trace shows a lengthy decrease (300 ns–500 ns) which includes multiple dips. During this noticeable decrease, the high voltage probe signal shows multiple peaks along with a lengthy tail. The lengthy decrease of the current trace occurs simultaneously with the multi-peak feature of all the X-ray signals gathered by the DXS system and is also accompanied by the multiple peaks of the high voltage probe.

The last peak of the X-ray signal appears 300 ± 50 ns after the first peak and its intensity and total duration is comparable with the first one. The total fluctuation time of the X-ray signals is around 300 ± 50 ns while the duration of each peak varies from 50 ns to 150 ns. The X-ray signals in the low range of operating pressure (0.4 mbar) are shown in Figs. 4(a) and 4(b). Comparing the signals gathered by the detectors with Cu, Co, and Ni filters indicates that the detector masked by a Cu filter experiences the highest intensity while the detector with a Co filter has the lowest intensity. At the best pinch condition, the intensity of the signals recorded by the detector with a Cu filter is 1.2 times larger than the ones gathered from the detector covered by a Ni filter, while the signals of the detector with a Ni filter are 3.5 times larger than the ones gathered by the detector covered by a CO filter. Comparing the signals of the detector masked alternatively with Al and Pb filters shows that signals of the detector when covered with Al have multiple discrete peaks, but when covered by a Pb filter, the detector does not reveal such a pattern in general.

The intensity of peaks in high voltage probe signals and the signals that are gathered from the detectors masked with Al or Pb show that there is a correlation between the peaks of X-ray signals and the intensity of the high voltage discharge. This correlation can also be observed for the signals of the detectors masked by Cu and Ni filters.

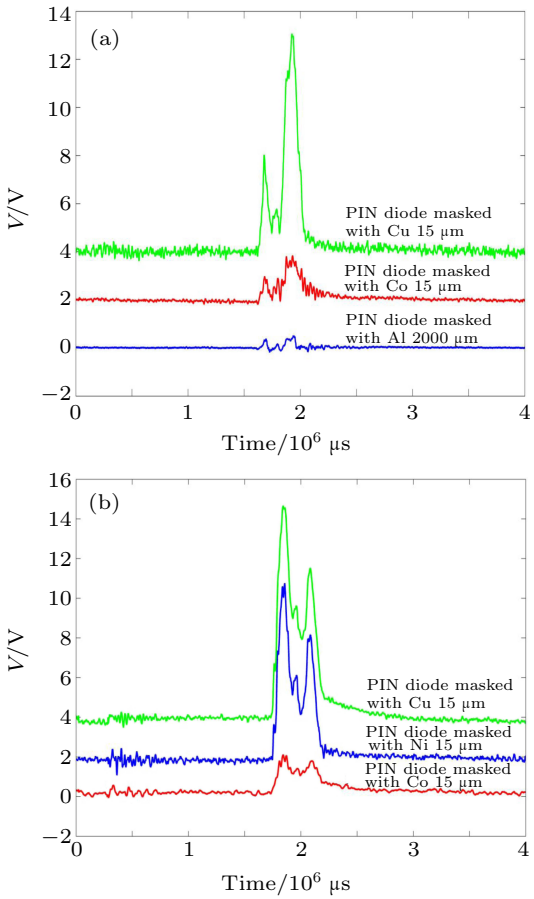


Fig. 4. (color online) (a) Typical multi-peak X-ray signal gained from the detectors masked by Cu (15 μm), Co (15 μm), and Al (2000 μm) filters. The operating pressure is 0.4 mbar (low range regime). (b) Typical multi-peak X-ray signal gained from the detectors masked by Cu (15 μm), Co (15 μm), and Ni (15 μm) filters. The operating pressure is 0.4 mbar.

4. Discussion

In a plasma focus system, the total energy ($E_{\text{total}} = (1/2)C_0V_0^2$) comes from the electric energy, initially stored in the capacitor bank (C_0) which is charged to a high voltage (V_0).

The tube voltage can be written as

$$V = V_0 - \frac{1}{C_0}\int_0^t I\,\mathrm{d}t - R_0 I - \frac{\mathrm{d}}{\mathrm{d}t}(L_0 I) = R_\mathrm{p} I_\mathrm{p} + \frac{\mathrm{d}}{\mathrm{d}t}\left(L_\mathrm{p} I_\mathrm{p}\right), \quad (1)$$

where I, I_p, R_p, L_0, and L_p are the total current, the plasma current, the circuit resistance, the plasma resistance, the fixed circuit inductance, and the charging voltage, respectively. Thus, the power input into the whole plasma system is

$$P_\mathrm{total} = I_\mathrm{p} V = I_\mathrm{p} L_\mathrm{p} \frac{\mathrm{d}I_\mathrm{p}}{\mathrm{d}t} + I_\mathrm{p}^2 \left(R_\mathrm{p} + \frac{\mathrm{d}L_\mathrm{p}}{\mathrm{d}t}\right). \quad (2)$$

Taking out the stored energy in the tube inductance, the power transferred into the plasma can be expressed as

$$P_\mathrm{plasma} = P_\mathrm{total} - \frac{\mathrm{d}}{\mathrm{d}t}\left(\frac{1}{2} L_\mathrm{p} I_\mathrm{p}^2\right) = I_\mathrm{p}^2 \left(R_\mathrm{p} + \frac{1}{2}\frac{\mathrm{d}L_\mathrm{p}}{\mathrm{d}t}\right). \quad (3)$$

The first term on the right-hand side of the equation indicates the induced Joule heating, which heats the plasma directly. The second term represents the power contributing to the dynamics of the system and the term $(1/2)(\mathrm{d}L_\mathrm{p}/\mathrm{d}t)$ can be interpreted as the "dynamic resistance, R_d" of the plasma.[29] Therefore, the total energy that has been transferred into the plasma (Energy Into Plasma, EINP) is

$$\mathrm{EINP} = \int_0^t I_\mathrm{p}^2 \left(R_\mathrm{p} + \frac{1}{2}\frac{\mathrm{d}L_\mathrm{p}}{\mathrm{d}t}\right) \mathrm{d}t. \quad (4)$$

One of the models that can describe some of the phenomena occurring in plasma focus devices is Lee's computational model based on the snowplow theory,[30] and it has been applied extensively and successfully for different devices.[31] This model couples plasma sheath dynamics, thermodynamics, and radiation with electric circuit equations to simulate the electrodynamic properties of the plasma focus. Recently, Lee introduced the concept of an anomalous resistivity effect[32,33] in the new version of his computational model (RadPFV.6).[34] The model has been considered for the design of a high static inductance (>100 nH) plasma focus device.[35] This new version assumes that different types of instabilities and microturbulences (anomalous resistivity effect) in the post pinch phase of anomalous resistance may play important roles in the consumption of energy by the plasma in these high inductance DPF machines.

During the radial phase, the amount of energy consumed by the plasma can be approximated as $(1/2)(L_\mathrm{p} I_\mathrm{pinch}^2)$,[31] and the energy stored in the magnetic field at the start of the radial phase can be expressed as $(1/2)(L_0 + L_\mathrm{a}) I_\mathrm{peak}^2$,[31] in which L_a is the axial inductance. In high static inductance plasma focus devices like the one in this experiment, the amount of L_p is much less than $(L_0 + L_\mathrm{a})$, hence the consumed energy is negligible compared to the energy stored in the magnetic field at the start of the radial phase. Therefore, there will be a considerable amount of stored energy, which can be consumed in the post-pinch phase of anomalous resistances.[34]

In Lee's computational model, the current and the tube voltage traces are the key data for interpreting the phenomena with or without considering the anomalous resistivity effect in a plasma focus device.[35] Lee's computational model was used without considering the anomalous resistivity effect. The computed current trace and tube voltage signals were fitted to typical measured ones. The result of the fitting, which is reported elsewhere,[36] revealed that for the best fitting parameters, the computed signals were not completely matched with the measured signals. Furthermore, the computational model could not explain the long decrease of the measured current along with the multi-peak pattern of the tube voltage signal. In another approach, the anomalous resistivity effect was introduced in a computational model,[37] which is formulated as

$$R = R[\exp(-t/t_2) - \exp(-t/t_1)], \quad (5)$$

where R_0 is a constant on the order of 1 Ω, t_1 is the characteristic rise time of the anomalous resistance, and t_2 is likewise the characteristic fall time. A parameter called "end fraction" was introduced in this model; it shows the termination of each anomalous resistance that appears as a dip on the measured current trace and separates them from each other. In Table 1, three anomalous resistances related to three dips on the measured current trace are tabulated.[36]

Table 1. Anomalous resistances used for the fitting process.

	R_0/Ω	t_1/ns	t_2/ns	end fraction
Dip 1	1.0	100	15	0.7
Dip 2	0.4	100	15	0.2
Dip 3	1.0	200	30	0.5

The results of the fitting process in the low range of operating pressure (0.4 mbar) are shown in Fig. 5.[36] As can be seen from the figure, there is good agreement between the measured and the computed signals. The anomalous resistance considered in the fitting can interpret the long decrease of the current trace along with its multi-dip feature, as well as, the multi-peak pattern of the high voltage probe signal.

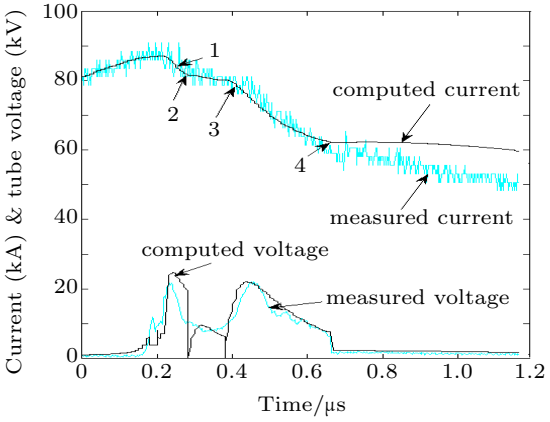


Fig. 5. (color online) The fitting process of measured and computed current traces along with high voltage probe signals for argon gas at 15 kV and 0.4 mbar. Number 1 is the end of the regular dip and numbers 2–4 are the ends of the first, second, and the third anomalous resistances, respectively. The zero point of the x axis is the start of the radial phase.

It is well known that anomalous resistance is responsible for the generation of energetic electrons and ions and emission of hard X-rays. In this machine, the appearance of multiple peaks in the X-ray signals, recorded by all four DXS channels, shows that the effect of anomalous resistance during the post-pinch phase must be responsible for the multi-radiation. The simultaneous long drop of the current trace and multi-peak pattern of the high voltage probe signal are yet another indication of the anomalous resistivity effect.[37] Lee *et al.* reported the results of a series of experiments regarding the correlation of measured soft X-ray pulses with modeled dynamics of the plasma focus.[38] They used the experimental results of the INTI-PF machine (2.2 kJ at 12 kV), which has an inductance of 114 nH and has parameters similar to the present experiment. They reported noticeable X-ray peaks that appear after the pinch, with energies higher than those that are characteristic of gas soft X-rays. From the analysis of the fitted current and the measured soft X-ray pulses, they concluded that the high energy soft X-ray pulses are correlated to the anomalous resistance phase and possibly because of the bremsstrahlung coming from the fully ionized plasma, which has been reported by others.[33]

In the present experiment, the analysis of the intensity, duration, and the number of peaks of Cu, Co, and Ni signals indicate that Cu–K_α makes a more significant contribution in the emitted X-ray spectrum than Cu–K_β, as is evident in the data recorded by the chosen set of filters. By applying the method of subtraction,[6] in the optimum pinch condition and in the side-on direction, X-rays in the form of Cu–K_α are emitted in the energy range of 0.14 ± 0.02 (J/Sr), and X-rays in the form of Cu–K_β are emitted in the energy range of 0.04 ± 0.01 (J/Sr). The significant portion of Cu–K_α and Cu–K_β are generated in the anomalous resistances phase.

The intensity and duration of the peaks in the signals recorded by an Al-masked detector show a significant contribution of multi-peaked X-rays with energies higher than 15 keV. The total estimated energy in the side on direction was approximately 0.12 ± 0.02 (J/Sr). The detection of high energy (higher than 15 keV) X-rays in this regime points to the generation of an energetic e-beam in the phase of anomalous resistances. By replacing the Al filter with Pb, it was demonstrated that the generation of multiple forms of X-rays with energy exceeding 30 keV is possible; however, the process cannot be repeated on a shot-to-shot basis. These findings are in accordance with the assessment of Lee *et al.*[38] that noticeable X-ray emission may occur during the post pinch phase of anomalous resistance.

5. Conclusion

In this article, the multi-radiation of X-rays and its correlation with the long drop of current trace and multiple peaks of the tube voltage was investigated based on the anomalous resistivity effect. The energy spectrum of the generated X-ray was studied using a special set of filters designed for the detection of medium and hard X-ray emission. The findings show that the anomalous resistivity effect during the post pinch phase can cause multi-radiation of X-rays with a significant contribution of Cu–K_α. The radiation can be categorized to be within the medium to hard range of X-ray emission with energies more than 15 keV and even more than 30 keV in some runs. By using the method of subtraction in the side one direction, the total emitted X-ray energy in the forms of Cu–K_α and Cu–K_β were around 0.14 ± 0.02 (J/Sr) and 0.04 ± 0.01 (J/Sr), respectively. The total energy of the emitted hard X-ray was estimated to be 0.12 ± 0.02 (J/Sr), which indicates emission of X-rays with energy more than 15 keV. The results reported here show that a significant portion of the total emitted X-rays in the form of Cu–K_α and Cu–K_β, as well as hard X-rays with energy > 15 keV, are generated during the anomalous resistances phase.

References

[1] Mohanty S R, Neog N K, Bhuyan H, Rout R K, Rawat R S and Lee P 2007 *Jpn. J. Appl. Phys.* **46** 3039
[2] Wong C S, Choi P, Leong W S and Singh J 2002 *Jpn. J. Appl. Phys.* **41** 3943
[3] Stygar W, Gerdin G, Venneri F and Mandrekas J 1982 *Nucl. Fusion* **22** 1161
[4] Kelly H and Marquez A 1995 *Meas. Sci. Technol.* **6** 400
[5] Patran A, Tan L C, Stoenescu D, Rafigue M S, Rawat R S, Springham S V, Tan T L, Lee P, Zakaullah M and Lee S 2005 *Plasma Sources Sci. Technol.* **14** 549
[6] Wong D, Patran A, Tan T L, Rawat R S and Lee P 2004 *IEEE Trans. Plasma Sci.* **32** 2227
[7] Rawat R S, Zhang T, Phua C B L, Then X Y, Chandra K A, Lin X, Patran A and Lee P 2004 *Plasma Sources Sci. Technol.* **13** 569
[8] Neog N K, Mohanty S R and Hotta E 2006 *J. Appl. Phys.* **99** 013302-1
[9] Neog N K, Mohanty S R and Borthakur T K 2008 *Phys. Lett. A* **372** 2294
[10] Verma R, Roshan M V, Malik F, Lee P, Lee S, Springham S V, Tan T L, Krishnan M and Rawat R S 2008 *Plasma Sources Sci. Technol.* **17** 04502
[11] Bortolotti A, Brzosko J S, Ingrosso I, Mezzetti F, Nardi V, Powell C and Robouch B V 1992 *Nucl. Instrum. Method Phys. Res. B* **63** 473
[12] Neff W, Eberle J, Holz R, Lebert R and Richter F 1989 *Proc. SPIE* 1140, November 27, 1989, Paris, France, p. 13
[13] Lee P, Feng X, Zhang G X, Liu M H and Lee S 1997 *Plasma Sources Sci. Technol.* **6** 343
[14] Mohanty S R, Sakamoto T, Kobayashi Y, Song I, Watanabe M, Kawamura T, Okino A, Horioka K and Hotta E 2006 *Rev. Sci. Instrum.* **77** 043506-1
[15] Dysan N A 1990 *X-rays in Atomic and Nuclear Physics* (Cambridge: Cambridge University Press)
[16] Vaughan D 1986 *X-ray Data Booklet* (Berkeley: Lawrence Berkeley Laboratory)
[17] Zakaullah M and Woreley J 2000 *J. Appl. Phys.* **85** 1251
[18] Ahmad S, Shafiq M, Zakaullah M and Waheed M 2006 *Appl. Phys. Lett.* **89** 061503
[19] Zakaullah M, Alamgir K, Shafiq M, Hassan S M, Sharif M and Waheed M 2001 *Appl. Phys. Lett.* **78** 877
[20] Shafiq M, Hussain S, Sharif M, Zakaullah M and Waheed A 2002 *Phys. Lett. A* **23** 302
[21] Shafiq M, Hussain S, Zakaullah M and Waheed A 2003 *Plasma Sources Sci. Technol.* **12** 199
[22] Hussain S, Zakaullah M, Ali S, Bhatti S H and Waheed A 2003 *Phys. Lett. A* **319** 181
[23] Hussain S, Shafiq M, Ahmad R, Waheed A and Zakaullah M 2005 *Plasma Sources Sci. Technol.* **14** 61
[24] Hussain S, Shafiq M and Zakaullah M 2010 *Appl .Phys. Lett.* **96** 031501
[25] Fillipov N V, Fillipova T I, Karakin M A, Krauz V I, Tykshaev V P, Vinogradov V P, Bakulin Y P, Timfeev V V, Zinchehenko V F, Brzosko J R and Brzosko J S 1996 *IEEE Trans. Plasma Sci.* **24** 1215

[26] Johnson D J 1974 *Rev. Sci. Instrum.* **45** 191

[27] Michette A G and Buckley C J 1993 *X-ray Science and Technology* (Bristol: Institute of Physics Publishing) p. 249.

[28] Henke B L, Gullikson E M and Davis J C 1993 *Atomic Data Nuclear Data Tables* "X-ray interactions: photoabsorption, scattering, transmission, and reflection at $E = 50$ eV–30000 eV, $Z = 1$–92" **54** pp. 181–342

[29] Lee S 2009 *Appl. Phys. Lett.* **95** 151503

[30] www.intimal.edu.my/school/fas/UFLF

[31] Lee S and Saw S H 2008 *Appl. Phys. Lett.* **92** 021503

[32] Bruzzone H 2001 *Nukleonika* **46** (supplement 1) 53

[33] Bernard A, Bruzzone H, Choi P, Chuaqui H, Gribkov V, Herrera J, Hirana K, Krejei A, Lee S, Luo C, Mezzetti F, Shadowski M, Schmidt H, Ware K, Wong C S and Zoita V 1998 *J. Moscow Phys. Soc.* **8** 93

[34] Lee S 2010 *Radiative Dense Plasma Focus Computation Pakage*: RADPF:

http://www.plasmafocus.net

http://www.plasmafocus.net/IPFS/modelpackage/File1RADPF.htm

http://www.plasmafocus.net/IPFS/modelpackage/File2Theory.pdf

http://www.plasmafocus.net/IPFS/modelpackage/UPF.htm

[35] Lee S, Saw S H, Abdou A E and Torreblanca H 2010 *J. Fusion Energy* **30** 277

[36] Behbahani R A and Aghamir F M 2011 *J. Phys. Plasmas* **18** 103302

[37] Behbahani R A and Aghamir F M 2012 *J. Appl. Phys.* **111** 043304

[38] Lee S, Saw S H, Rawat R S, Lee P, Talebitaher A, Abdou A E, Chong P L, Roy F A, Singh A, Wong D and Devi K 2011 *IEEE Trans. Plasma Sci.* **39** 3196